# A self-monitoring strategy for TRIME Time Domain Reflectometry moisture sensors

Nicholas Tan Jerome
*Research & Development*
*IMKO GmbH*
Ettlingen, Germany
nicholas.tanjerome@imko.de

***Abstract*—Time Domain Reflectometry ( TDR) i s w idely used to determine the water content of porous media. However, the raw TDR signal is susceptible to electromagnetic interference (EMI) that can lead to faulty measurements. I developed a self-monitoring strategy for real-time data evaluation that is applied in TRIME TDR sensors, in which the strategy can also be adapted to other conventional TDR sensors. The self-monitoring strategy combines moving variance and Pearson correlation methods to improve data integrity. Particularly, the strategy helps to avoid undetectable false measurements and eases the complexity of filter i mplementation w ithin t he sensor. In evaluations, I examined the influence o f t he E MI, between $100\,\mathrm{kHz}$ to $6\,\mathrm{GHz}$, on TRIME TDR sensors under conducted and radiated disturbances induced by radio-frequency fields according to the IEC 61000-4-3 and the IEC 61000-4-6 standards. Finally, the measurement fluctuation i s s ignificantly improved resulting in a data tolerance of lower than $4\,\%$ under induced radio-frequency disturbances.**

***Index Terms*—Time Domain Reflectometry, E MI Detection, Application, Real-time Data Analysis**

## I. Introduction

The determination of water content is the key parameter to maintain the quality of goods and materials. Hence, there is a trend of deploying Time Domain Reflectometry (TDR) systems as part of the automated process in industrial applications [1]–[3]. A TDR measurement is based on the analysis of the reflected s ignal, w here t he t otal t ime o f s ignal traveled along the waveguide (sensing probe) is measured. When a signal or TDR pulse propagates along the waveguide, energy dissipation or dielectric loss occurs that affects the shape of the reflected s ignal r egarding t he s ignal's t ravel t ime a nd the signal's amplitude. Depending on the medium surrounding the waveguide, the reflected s ignal c an i nfer t he w ater content within the medium [4].

However, electromagnetic interference (EMI) noise can affect the sensor circuits by inducing voltages on conductors, where the sensor's waveguide becomes an unintentional antenna that captures the EMI radiation [5]. There are two categories of EMI noise: intentional and unintentional. On the one hand, unintentional EMI sources such as lightning strikes, electric trains, transformers, and radios are known to interfere with modern circuits and sensors [6]–[8]. On the other hand, intentional EMI can disrupt electronic components and can inject signals to falsify the sensor values [5]. Tedeschi et al. studied the effects of EMI noise to the TDR measurement [9]. In particular, they reviewed the performance of the Spread Spectrum Time Domain Reflectometry (SSTDR) system [10], where SSTDR is mainly used to monitor live conductor fault in a noisy environment. Although there is no mention of using the SSTDR as a moisture sensor, it is worth noting that the SSTDR is a TDR system with high noise immunity [10]. The reason is due to the use of pseudorandom noise and spread spectrum frequencies, which is similar to the direct sequence spread spectrum (DSSS) approach [11]. Despite SSTDR being a noise-resistant TDR system, this approach requires dedicated electronics such as correlator and modulator. My approach will be based on solely studying the raw data of a TDR system without hardware extension, and it is generally applicable to any TDR system.

In this paper, I study the effects of intentional EMI noise on TDR sensors. I present a self-monitoring strategy that can identify corrupted TDR signal based on the signal integrity of TDR parameters. The strategy detects the EMI by using the Pearson correlation and the moving variance methods by correlating two primary TDR parameters: the voltage level and the water content. To evaluate the effectiveness of the proposed strategy, I study the data fluctuation of a defined water content using the EMI noise spectrum according to the IEC 61000-4-3 and IEC 61000-4-6, where the TRIME TDR sensor is subjected to radio-frequencies from $100\,\mathrm{kHz}$ to $6\,\mathrm{GHz}$.

## II. Background

A typical TDR setup consists of a pulse generator (transmitter), a transmission line (sensing probe), and an oscilloscope (receiver). The receiver component performs a time-based sampling on the reflected signal to determine the signal's travel time. Alternatively, the TRIME [1] technology performs a voltage-based sampling [12]–[14] that scans the reflected signal by its voltage axis. The voltage sampling approach simplifies the TDR system where the display component is omitted, resulting in a small compact chip. Figure 1 shows the block diagram of the TRIME TDR system, where timestamps C and D represent the travel time of the TDR signal. In a different medium, the timestamp D will vary according to its dielectric constant and water content [15].

[1]TRIME stands for Time Domain Reflectometry with Intelligent Micro-module Elements.

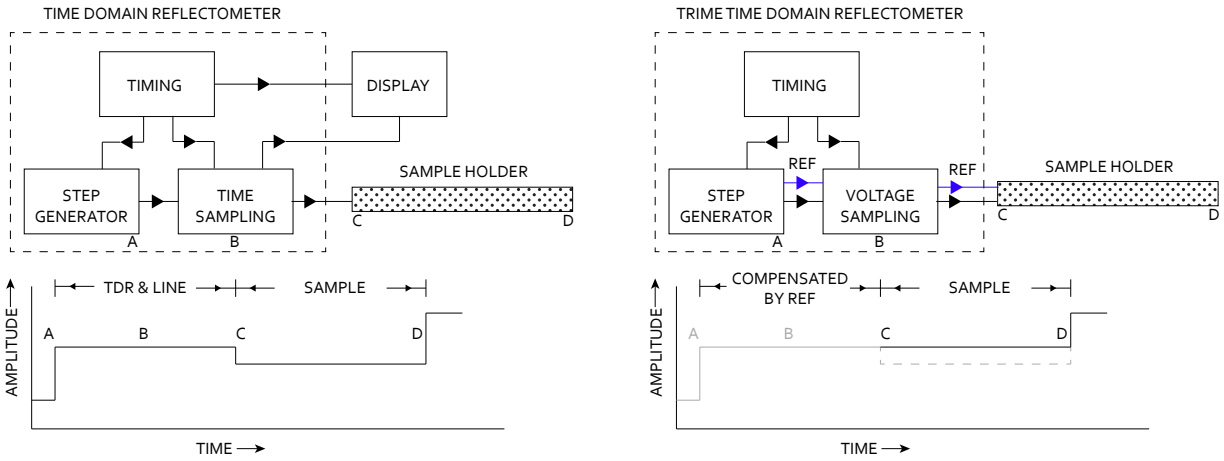


(a) Conventional TDR [4]

(b) TRIME TDR [12]

Fig. 1: A block diagram of TDR connected to the sample holder (top), and an idealized representation (amplitude vs time) of the conventional and TRIME TDR outputs (bottom). The blue line depicts the reference line (REF) that helps to compensate the unwanted section.

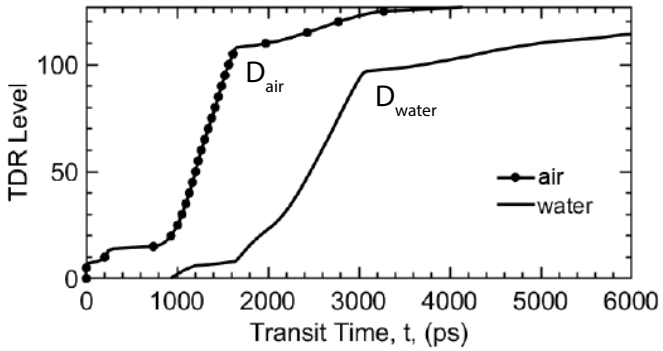


Fig. 2: Two typical TRIME TDR signals that measure air and water. D represents the rising edge of the signal which is the total time taken for a round trip of the TDR signal.

Figure 2 shows that the timestamp D for water, $D_{water}$, is longer than the timestamp D of air, $D_{air}$. $C$ depicts the start of the waveguide, and $D$ represents the round trip of the propagated signal. Thus, the travel time of the signal is the difference between $D$ and $C$ ($t = D - C$). For sensors with an integrated sensor probe, $C$ is negligible ($t \approx D$). We can determine the travel time of the signal by deriving the apparent dielectric constant ($\epsilon_a$) using Equation 1.

$$\epsilon_a = \left(\frac{c}{v}\right)^2 = \left(\frac{ct}{2L}\right)^2 \tag{1}$$

where $c$ is the speed of light and $t$ is the travel time along the transmission line with a length, $L$. $v$ is the velocity of the signal. Hence, we can infer the water content ($\theta$) of the material from the apparent dielectric constant ($\epsilon_a$) by using a third-order polynomial equation [16].

$$\begin{aligned}\theta = &- 5.3 \times 10^{-2} + 2.92 \times 10^{-2}\epsilon_a \\ &- 5.3 \times 10^{-4}\epsilon_a^2 + 4.3 \times 10^{-6}\epsilon_a^3\end{aligned} \tag{2}$$

Figure 2 shows two typical TRIME TDR signals measured in the air and the water. The Y-axis denotes the discrete step of the analog-digital-converter (ADC), $N$, which is represented as the TDR LEVEL. The instantaneous ADC voltage, $V_i$, can be derived using the equation:

$$V_i = (V_H - V_L) * N \tag{3}$$

where $V_H$ and $V_L$ represent the upper and lower voltage limit of the ADC window. $N$ describes the ADC discrete step. In this paper, I will use the term *TDR Level* to represent the ADC voltage level of the TRIME TDR signal , and the term *moisture* to describe the water content within a material. The water content is derived from the travel time of the TDR signal.

## III. Test Setups

To study the influence of EMI noise on a TDR sensor, I evaluated conducted and radiated disturbances induced by radio-frequency fields according to IEC 61000-4-3 and IEC 61000-4-6 procedures, which covers the frequencies between 100 kHz and 6 GHz. The two standard procedures are electromagnetic compatibility standards that allow test reproducibility (Figure 3). The conducted disturbances cover the frequencies between 100 kHz and 80 MHz, whereas the radiated disturbances cover the frequencies between 80 MHz and 6 GHz. Since the data fluctuation is observed even at a low electric field strength of 1 V/m, I decided to conduct these tests with a higher nominal field strength at 12 V/m.

In this study, I used TRIME SONO-VARIO to represent a TDR sensor (Figure 4). The sensor is placed on top of a polystyrene container that contains glass beads with a water content of 17 %. If there are no disturbances on the

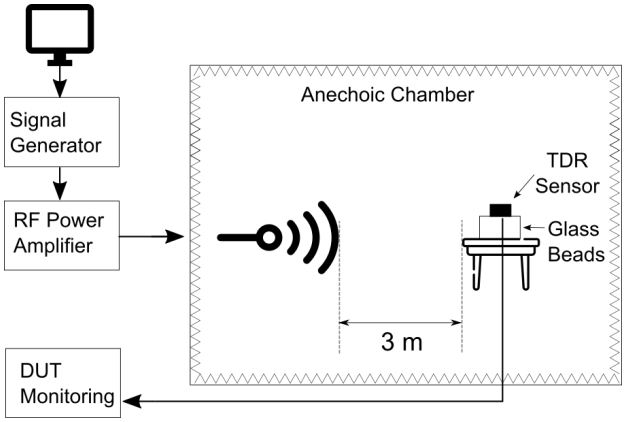


(a) IEC 61000-4-3: Radiated Interference, RI (0.08 GHz to 6 GHz)

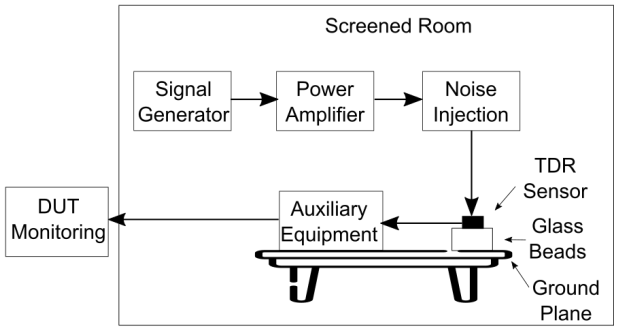


(b) IEC 61000-4-6: Conducted Interference, CI (0.1 MHz to 80 MHz)

Fig. 3: Test setups based on electromagnetic compatibility standard procedures. DUT: device under test. These standards are chosen for test reproducibility purpose.

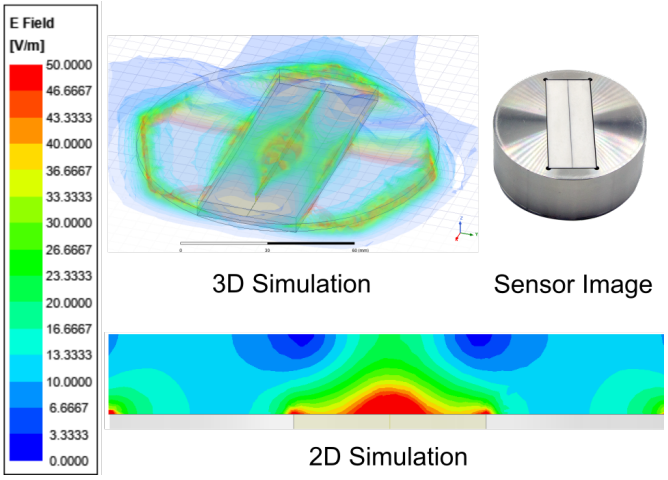


Fig. 4: TRIME SONO-VARIO, a Time Domain Reflectometry sensor. The 2D and 3D simulations are created by using the Ansys HFSS software which show the elctromagnetic field distribution of the sensor. The simulation snapshots are taken at the time step of 800 ps.

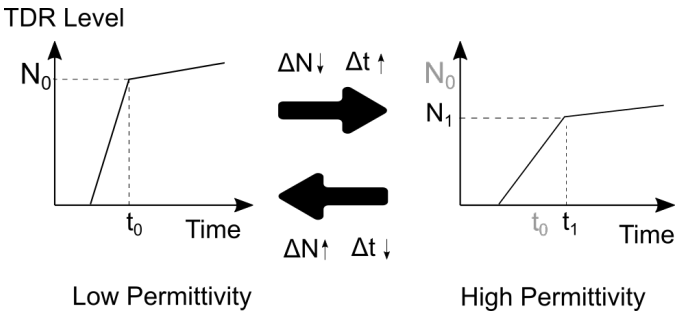


Fig. 5: The relationship of the TDR signal when moving from low to high permittivity, and vice versa, where the difference of TDR Level, $\Delta N$, is inversely proportional to the difference of travel time, $\Delta t$, of the TDR signal.

TDR signal, we should expect the same water content value throughout the broad EMI noise spectrum. Also, I disabled data processing filters within the sensor to emphasize the raw TDR signal.

## IV. Method

To differentiate between good and faulty TDR signals, I compare the two main TDR parameters (TDR Level and travel time) while transitioning between two different permittivity states. For example, increasing amount of water in a bulk material can lead to higher bulk permittivity, which results in lower TDR Level and higher travel time of the TDR signal and vice versa (Figure 5). While considering the transition between two permittivity states, the change of the TDR Level value is inversely proportional to the change of the travel time value. The water content is then derived from the travel time based on the Equation 2.

To quantify this relationship, I propose the moving Pearson correlation approach that correlates the buffered water content measurements with the buffered measured TDR Level measurements. The Pearson correlation approach is chosen due to its simplicity.

Figure 6 shows the self-monitoring strategy that identifies invalid data. Initially, measured water content and TDR level are grouped into ring buffers (FIFO), where the buffers serve as the input data of the monitoring process. Each ring buffer consists of $n_d$ elements that determines the response time of a monitoring process. In real-world applications, water content and TDR level parameters do not correlate positively, unless when it is a static measurement where both parameters are constant (static data). To identify the correlation between the two TDR parameters and also the static data, I combine Pearson correlation, $c_p$, together with a data variance evaluation to study the relationship between the two distinct

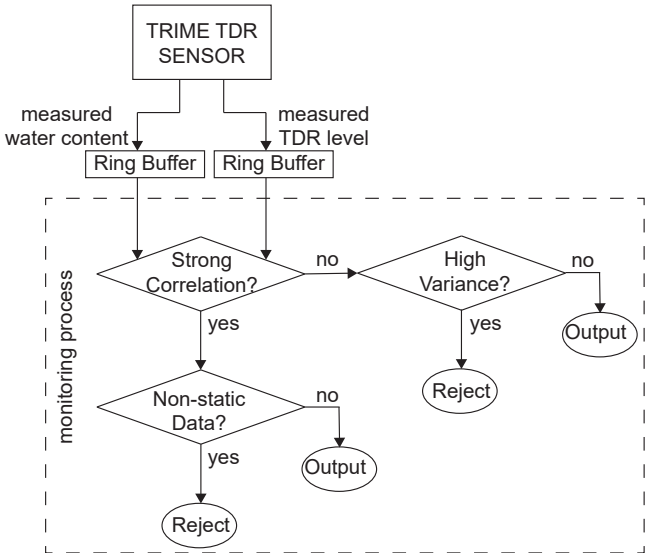


Fig. 6: Self-monitoring strategy for the TRIME TDR sensor.

parameters. On the one hand, if both parameters correlate strongly and positively ($c_p > T_c$), the data variance will then be evaluated where high data variance suggests the presence of EMI (reject), and low data variance suggests a static measurement phenomenon (valid output). On the other hand, when both parameters correlate weakly ($c_p < T_c$), the data variance will be evaluated where measurements with high data variance will be rejected. The high data variance is defined by setting a threshold, $T_{hv}$. The low data variance is defined as the data variance of the ring buffer does not exceed the threshold $T_s$.

## V. Results and Discussion

In the evaluation, I selected the following parameters: $n_d = 6$, $T_c = 0.8$, $T_{hv} = 50$, $T_s = 1$. These parameters are carefully selected after comparing with data sets of intentional EMI, together with the data sets from various real-world moisture measurement applications: corns, concrete aggregates, wood chips, wood shavings, sand, and sewage sludge. The selected parameters should ensure only data rejection under the affect of EMI noise. The proposed strategy is tested against the measurement data in the EMC laboratory. Also, I presented two real-world applications to validate the effectiveness of the strategy.

### A. Measurement Results in the EMC Laboratory

In both procedures, I observed high data fluctuations that distort the measurement output (The correct water content value should be at 17 %). On the one hand, in the conducted disturbance mode, the data fluctuation begins at 20 MHz onwards; on the other hand, in the radiated disturbance mode, the data fluctuation occurs between 0.08 GHz to 3.5 GHz.

By applying the proposed strategy into the TRIME TDR sensors, many data points under the influence of EMI are rejected (red), in which the valid data points (blue) have a

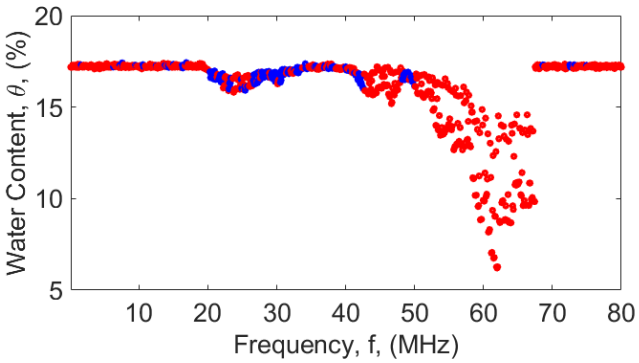


Fig. 7: Conducted Interferences (0.1 MHz to 80 MHz). Maximum: 17.51 %, Minimum: 15.92 %, Difference: 1.59 %. The lower the difference value, the better. Blue points depict good values, whereas red points depict rejected values.

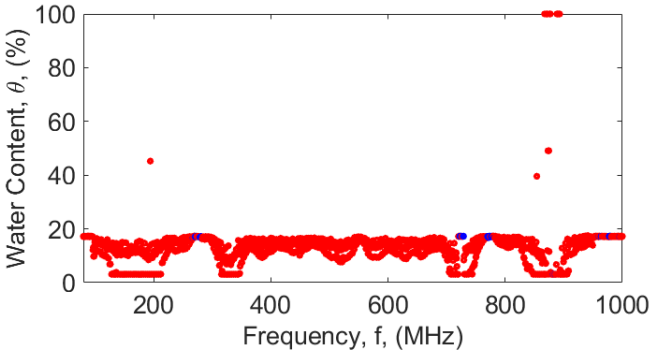


Fig. 8: Radiated Interferences (80 MHz to 1000 MHz). Maximum: 17.34 %, Minimum: 16.34 %, Difference: 1.00 %. The lower the difference value, the better. Blue points depict good values, whereas red points depict rejected values.

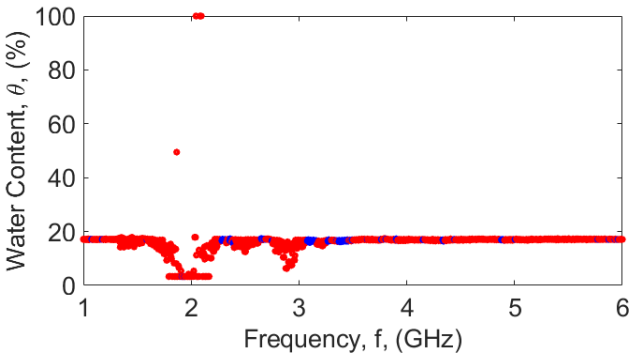


Fig. 9: Radiated Interferences (1 GHz to 6 GHz). Maximum: 17.28 %, Minimum: 14.04 %, Difference: 3.24 %. The lower the difference value, the better Blue points depict good values, whereas red points depict rejected values..

data fluctuation less than 3.24 %, as shown in Figure 7, 8 and 9. There is a caveat in performing the proposed strategy. If the measured water content is limited between 0 % and 100 %, the

approach will not consider TDR travel times beyond the water content limits. However, under the EMI, the measured travel times fluctuation may go beyond the limited range, resulting in a series of false static values at $0\,\%$ or $100\,\%$. In this case, it is worth considering to substitute the water content value with the TDR travel time parameter in the monitoring strategy, where the travel time parameter is unbounded.

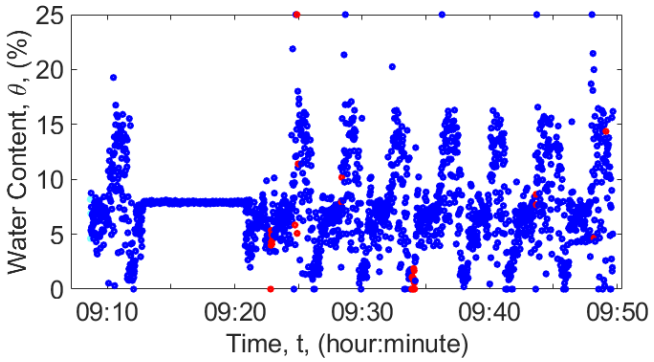


Fig. 10: The water content values in the concrete mixer. The blue points represent good values (2117 points), whereas the red points represent the rejected values (40 points).

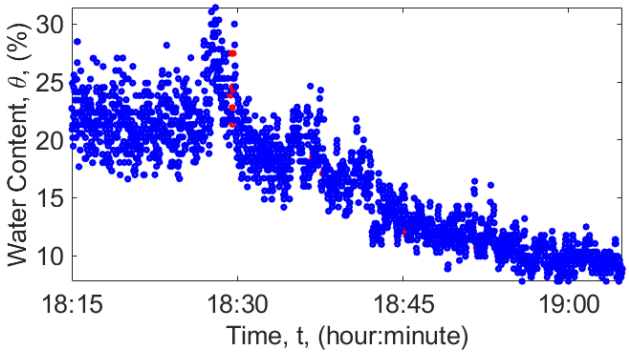


Fig. 11: The water content values in the wood chip dryer. The blue points represent good values (2219 points), whereas the red points represent the rejected values (12 points).

### *B. Measurement Results in the Concrete Mixer and the Wood Chip Dryer*

Although the water content values within a concrete mixer and the wood chip dryer fluctuates continuously (noisy and dynamic systems), every measured data should be valid. To test the feasibility of the proposed strategy, the measured data should not be rejected. Figure 10 shows the water content values in the concrete mixer that uses the strategy to distinguish the measurement validity. There are 40 invalid values from the total 2117 values which results in a reject ratio of $1.8\,\%$. Figure 11 shows the water content values in the wood chip dryer, where there are 12 invalid values from a total of 2231 values which results in a reject ratio of $0.5\,\%$. The low reject ratios prove the feasibility of the proposed strategy, where it detects the EMI while preserving the TDR values in normal operations.

## VI. Conclusion

The combination of Pearson correlation and moving variance allows an efficient self-monitoring for TRIME TDR sensors. As shown experimentally in this paper, we can improve the robustness of existing TDR systems by having a data fluctuation of less than $4\,\%$ (with raw data and under EMI). Performing further data filtering on the output values such as Kalman filtering, we can expect a data fluctuation of less than $1\,\%$. The proposed strategy is tested in different applications such as in the concrete mixer and the wood chip dryer, where the low reject ratios shows the credibility of the strategy to filter out invalid TDR values.

## References


[1] A. Cataldo, E. De Benedetto, G. Cannazza, E. Piuzzi, and E. Pittella, "Moisture content monitoring of construction materials: From in-line production through on-site applications," in *2017 IEEE International Instrumentation and Measurement Technology Conference (I2MTC)*, pp. 1–5, IEEE, 2017.

[2] S.-G. Lee, K.-S. Kwon, B.-J. Kim, N.-C. Choi, J.-W. Choi, and S. Lee, "Detection of oil leakage in soil by monitoring impedance using time domain reflectometry and hydraulic control system," *Process Safety and Environmental Protection*, 2019.

[3] N. Hager III and R. Domszy, "Monitoring of cement hydration by broadband time-domain-reflectometry dielectric spectroscopy," *Journal of applied physics*, vol. 96, no. 9, pp. 5117–5128, 2004.

[4] G. C. Topp and W. D. Reynolds, "Time domain reflectometry: A seminal technique for measuring mass and energy in soil," *Soil and Tillage Research*, vol. 47, no. 1-2, pp. 125–132, 1998.

[5] D. F. Kune, J. Backes, S. S. Clark, D. Kramer, M. Reynolds, K. Fu, Y. Kim, and W. Xu, "Ghost talk: Mitigating emi signal injection attacks against analog sensors," in *2013 IEEE Symposium on Security and Privacy*, pp. 145–159, IEEE, 2013.

[6] D. Mansson, R. Thottappillil, and M. Backstrom, "Methodology for classifying facilities with respect to intentional emi," *IEEE Transactions on electromagnetic compatibility*, vol. 51, no. 1, pp. 46–52, 2009.

[7] J.-M. Redouté and M. Steyaert, *EMC of analog integrated circuits*. Springer Science & Business Media, 2009.

[8] C. R. Paul, "Electromagnetic compatibility," *Encyclopedia of RF and Microwave Engineering*, 2005.

[9] J. R. Tedeschi, L. E. Smith, R. C. Conrad, G. Gavric, M. A. Zalavadia, D. T. Keller, and R. M. Pratt, "Active time-domain reflectometry for unattended safeguards systems: Fy16 report," tech. rep., Pacific Northwest National Lab.(PNNL), Richland, WA (United States), 2016.

[10] P. Smith, C. Furse, and J. Gunther, "Analysis of spread spectrum time domain reflectometry for wire fault location," *IEEE sensors journal*, vol. 5, no. 6, pp. 1469–1478, 2005.

[11] D. Torrieri, *Principles of spread-spectrum communication systems*, vol. 1. Springer, 2005.

[12] M. Stacheder, R. Fundinger, and K. Koehler, "A new time domain reflectometry system (TRIME) to measure soil moisture and electrical conductivity," in *Symposium and workshop on time domain reflectometry in environmental, infrastructure, and mining applications*, pp. 56–65, 1994.

[13] K. Köhler, "Apparatus for determining the moisture content of a medium," Sept. 14 2004. US Patent 6,792,362.

[14] K. Kohler and R. Fundinger, "Apparatus for determining the moisture content of a medium," Oct. 17 1995. US Patent 5,459,403.

[15] D. Robinson, M. Schaap, D. Or, and S. B. Jones, "On the effective measurement frequency of time domain reflectometry in dispersive and nonconductive dielectric materials," *Water Resources Research*, vol. 41, no. 2, 2005.

[16] G. C. Topp, J. Davis, and A. P. Annan, "Electromagnetic determination of soil water content: Measurements in coaxial transmission lines," *Water resources research*, vol. 16, no. 3, pp. 574–582, 1980.